I&EC research
Industrial & Engineering Chemistry Research

ARTICLE

pubs.acs.org/IECR

Monitoring the Ozonation of Phenol Solutions at Constant pH by Different Methods

Edgardo M. Contreras,*[,†,‡] Nora C. Bertola,[†,§] and Noemi E. Zaritzky[†,‡]

[†]Centro de Investigación y Desarrollo en Criotecnología de Alimentos (CIDCA) CCT La Plata CONICET - Fac. de Cs. Exactas, UNLP, 47 y 116 (B1900AJJ) - La Plata, Argentina

[‡]Fac. de Ingeniería, UNLP, 47 y 1 (B1900AJJ) - La Plata, Argentina

[§]Fac. de Ciencias Exactas, UNLP, 47 y 1 (B1900AJJ) - La Plata, Argentina

ABSTRACT: In this study the oxidation−reduction potential (ORP) and the proton production (Hp) profiles as a function of time were proposed as indicators to monitor the ozonation of phenol solutions at constant pH. Analysis of the ozone gas outlet stream (X_{O3}), COD, and phenol measurements in the aqueous phase confirm the reliability of the proposed indicators. Results show that the derivative with respect to time of the normalized ozone gas outlet concentration ($(1/X_{O30})dX_{O3}/dt$), of the oxidation−reduction potential ($dORP/dt$) or of its logarithmic value ($dLog(ORP)/dt$), and of the proton production rate (dHp/dt) exhibited maximum values that were close to the critical ozonation time (t_c) determined by X_{O3}, COD, and phenol measurements. Additionally, ORP and X_{O3} measurements were useful to determine t_c for all the tested pHs (5 to 11); however, Hp was useful only for pH values higher than 9. The indicators of the ozonation process proposed in the present work (ORP, Hp) as alternatives of X_{O3} may be useful to control the addition of ozone, minimizing the ozonation process costs.

1. INTRODUCTION

Phenol, phenolic compounds, and its derivatives are major environmental pollutants from industrial processes such as petroleum processing plants, oil refineries, coke ovens, and pharmaceutical industries. The largest use of phenol is as an intermediate in the production of phenolic resins, synthetic fibers, and for epoxy resin precursors. Besides, phenol is naturally present in some foods, in human and animal wastes, in decomposing organic material, and is produced endogenously from the metabolism of protein.[1]

As environmental regulations become more restrictive, innovative treatments of wastewaters containing phenols must be considered. Phenols can be removed from industrial wastewaters by biological or physicochemical methods. Usually, the application of biological methods is limited to nontoxic biodegradable wastewaters. To reduce its toxicity, a pretreatment of industrial wastewaters is necessary. Among physicochemical methods to treat industrial wastewaters, advanced oxidation processes (AOPs) are often chosen. Phenols can be removed from industrial wastewaters by AOPs such as ozonation, Fenton reaction, UV, or hydrogen peroxide.[2,3] Ozone is one of the most used AOPs; however, the major drawbacks concerning the use of ozone are related to the high costs associated with the water ozonation facilities and to the generation of ozone.[4]

The utilization of ozone for treating wastewaters containing phenolic compounds emphasizes the practical requirement for developing adequate mathematical models to be used for the design and operation of these processes. Extensive studies have been performed regarding the ozone self-decomposition mechanism in water,[5−8] and the reaction pathway of the phenol oxidation by ozone under different conditions.[9−11] In general, aromatic rings are prone to react directly with ozone while saturated hydrocarbons, alcohols, aldehydes, etc., are considered resistant to ozone attack. In the latter case, indirect (free radical) reactions might play a significant role; however, the importance of these indirect reactions also depends on the concentration of fast ozone-reacting compounds, the concentration of hydroxyl radicals, the presence of initiators, promoters and inhibitors of free radicals, and pH of the wastewater.

When a phenol-containing wastewater is oxidized by ozone, in most cases, two reaction periods are usually observed.[12] The first period comprises a fast decrease of the concentration of pollutants (expressed in COD units, for example) coupled with a high ozone consumption rate; this period is related to the electrophilic attack of ozone to aromatic rings, resulting in more oxidized aromatic compounds (catechol, resorcinol, hydroquinone, benzoquinone, etc.) and open ring compounds, such as muconic acid.[9,13,14] Then, when the pollutants concentration is below a certain critical value, ozone consumption rate continuously decreases until it eventually stops. In this second period occurs the oxidation of saturated hydrocarbons, alcohols, and aldehydes resulting in simple carboxylic acid, such as oxalic, malic, formic, and fumaric, via indirect (free radical) reactions.[10,11,14] The formation of aldehydes as ozonation byproducts is of particular concern because they are potentially carcinogenic and mutagenic. Recently, Silva et al.[15] demonstrate the formation of formaldehyde, acetaldehyde, glyoxal, and methylglyoxal during the ozonation of an anaerobic sanitary wastewater. Petala et al.[16] showed that the application of low ozone doses induced a decrease of toxicity of a secondary municipal wastewater, whereas ozone doses higher than 5.0 mg O_3 L^{-1} resulted in an

Received: May 9, 2011
Accepted: July 12, 2011
Revised: July 5, 2011
Published: July 12, 2011

dx.doi.org/10.1021/ie200999h | *Ind. Eng. Chem. Res.* 2011, 50, 9799–9809

increase of toxicity due to the formation of toxic ozonation byproducts.

The determination of the critical ozonation time (the process time at which ozone and COD consumption rates drastically decrease) has important implications in actual ozonation facilities. For example, an optimized industrial wastewater treatment process could comprise the combination of an ozonation step until the critical ozonation time, followed by a biological treatment.[17,18] After the critical ozonation time, the concentrations of fast ozone reacting compounds (e.g., aromatic rings) are low, thus, the oxidation rate decreases and the ozonation process becomes less effective. In addition, compounds obtained at the end of the first period of ozonation are usually readily biodegradable, and therefore, they are suitable for a biological treatment. Unfortunately, the unknown nature and concentration of pollutants in actual wastewaters constitutes the main problem for predicting the critical ozonation time.

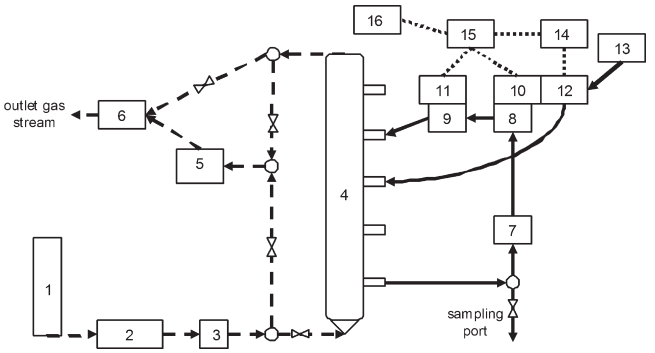

Figure 1. Experimental setup: (1) oxygen cylinder, (2) ozone generator, (3) gas flow meter, (4) bubbled column, (5) ozone gas meter, (6) KI trap, (7) recirculation pump, (8) pH probe, (9) ORP probe, (10) pH controller, (11) ORP meter, (12) NaOH pump, (13) NaOH buret, (14) optocoupler (15) A/D converter, and (16) PC. Continuous lines indicate liquid streams, dashed lines indicate gaseous streams, and dotted lines depict the connections between measurement modules.

To minimize ozonation costs associated with ozone generation and energy savings, monitoring devices capable of measuring ozone concentration in the gas phase have been developed.[4] The presence of a given ozone level in the outlet gas phase of an ozone reactor indicates that the ozone demand of the wastewater has been satisfied. If the ozone gas concentration increases, it means that excess of ozone is being generated. This approach to control the ozone generation is based on the reliability of the ozone gas phase measuring device. In general, ozone detectors are relatively expensive.[19] Most commercially available ozone monitors are based on the light absorption at 254 nm by gaseous ozone. These monitors have several drawbacks such as the baseline drift, and the interference from nitric oxides, hydrogen peroxide, nitric acid, and volatile organic compounds that are usually found in the outlet gas of an ozone contactor.[20] Recently, other monitors such as electrochemical or heated metal oxide ozone sensors were developed; these sensors are subject to critical interferences (including volatile organic compounds and humidity) and also suffer from accuracy problems.[19−22] For this reason, alternative indicators of the ozonation process are necessary to control the addition of ozone, as well as to minimize ozonation costs.

The objective of this work was to study the suitability of different methods to determine the critical ozonation time (t_c)

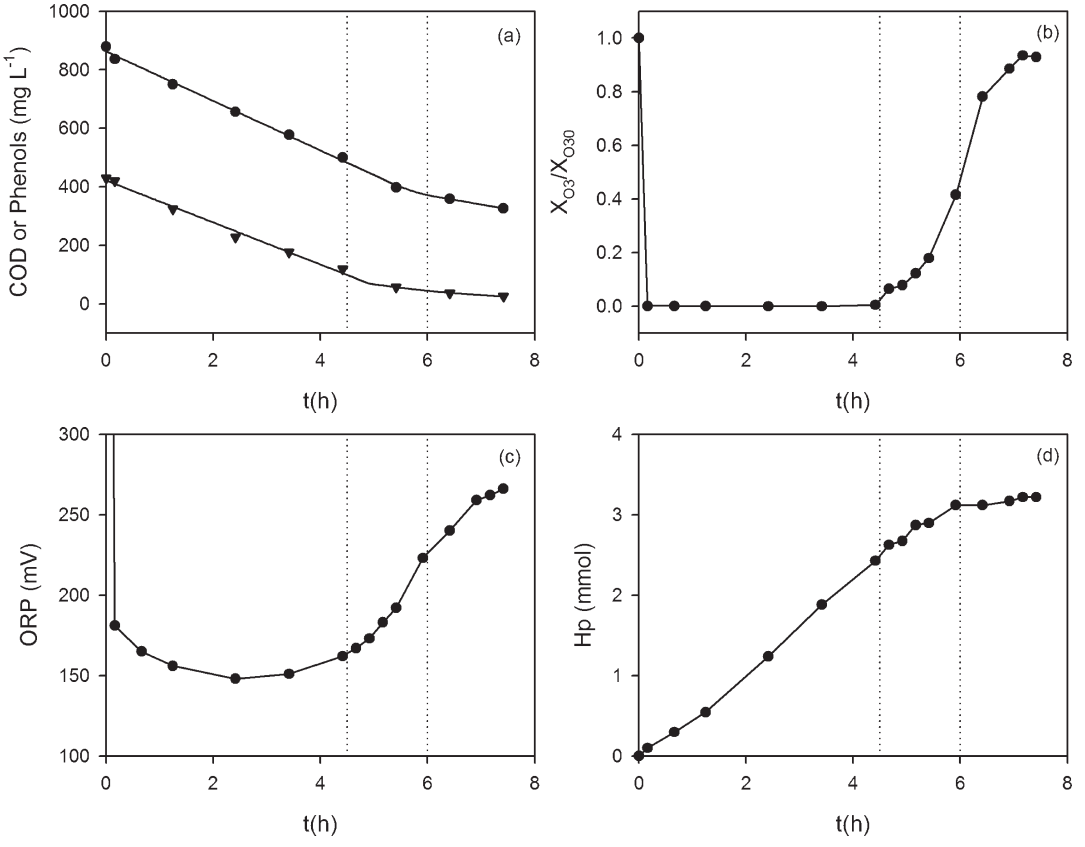

Figure 2. Time profiles of (a) COD (●), phenols (▼), (b) normalized ozone gas outlet concentration, (c) oxidation−reduction potential (ORP), and (d) proton production (Hp). Dotted lines indicate the time interval corresponding to the critical ozonation time.

of phenol solutions at constant pH. The proposed methods were based on the changes observed on the oxidation−reduction potential (ORP) or the proton production (Hp) during the ozonation process. In addition, an electrochemical ozone gas sensor, COD, and phenol measurements in the aqueous phase were employed to contrast the reliability of the proposed methods.

2. MATERIALS AND METHODS

2.1. Chemicals. Phenol (loose crystals, > 99%) was obtained from Sigma (St. Louis, MO, USA) and used without further purification. All inorganic salts were commercial products of reagent grade from Anedra (San Fernando, Argentina). Distilled water was used to prepare all the solutions used in the present work.

2.2. Experimental Setup. Ozonation of phenol solutions was conducted in a bubble column (33 mm i.d. × 1100 mm total height) with a maximum working volume of 800 mL (Figure 1). Pure oxygen (0.5 L min^{-1}) was used to feed a corona discharge ozone generator (O_3 Zex, Henz Argentina); ozone mass flow rate was F_{O3} = 59 ± 3 mgO_3 h^{-1}, at 1 atm and 25 °C. The oxygen/ozone gas mixture was introduced by passing through a sintered glass diffuser installed at the bottom of the column. A stable gas flow rate was obtained (0.5 L min^{-1}) using a high-precision rotameter (Bruno Schilling model MB 60 V, Argentina). Ozone concentration in the gaseous outlet stream (X_{O3}) was measured using an electrochemical ozone sensor (Xilix model DCM IV, Argentina); a potassium iodide (KI) trap was used to eliminate the excess of ozone.

An external recirculation line by a peristaltic pump (Apema model AP20, Argentina) from the bottom to the top of the column was used to achieve homogeneous mixing of the solution; in all experiments the recirculation flow rate was 230 mL min^{-1}. Oxidation−reduction potential (ORP) and pH of the recirculation line were measured continuously using polymer body probes (Broadley-James Corp., USA). The pH monitor was connected to an on/off pH controller module (Masstek, Argentina); pH of the column was corrected (±0.02 units) by adding NaOH (0.25 M) via a peristaltic pump (Apema model AP20, Argentina). An 8-bit A/D converter (Biloba Ingenieria model BLB 2.0, Argentina) was used to obtain the output signal (4−20 mA) from ORP and pH monitors. The on/off control signal actuating the NaOH pump (Apema model AP25 0.3-M-S) was converted to 250 mV or null signal via an optocoupler connected to the A/D converter module (Biloba Ingenieria, Argentina); the A/D converter module was connected to a personal computer via an RS232 protocol. This device allowed measuring the cumulative pumping time to maintain the pH value at a constant set point through the addition of a NaOH solution. If the flow rate of the peristaltic pump is constant, then the cumulative pumping time is proportional to the added volume. The total proton production (Hp) as a function of the process time can be calculated as the product between the added volume and the concentration of NaOH. Because some of the phenol oxidation products by ozone are carboxylic acids, pH tends to decrease as the ozonation proceeds. If pH is maintained constant due to the addition of an alkali, the amount of NaOH added must be equal to the amount of protons released due to the formation of acids during the ozonation process. More details concerning titrimetry methods to monitor reactions can be obtained in Contreras.[23]

Ozonation of phenol solutions was performed as follows: 500 mL of a phosphate buffer solution (8.5 mM, pH = 7) was poured into the column. Then, oxygen flow rate was set to 0.5 L min^{-1} and the ozone generator was turned on. When stable ORP, pH, and ozone concentration in the gas outlet stream measurements were achieved, a pulse of phenol was introduced using a syringe at the middle height of the column. Tested initial phenol concentrations (Ph_0) were 150, 210, and 420 mg L^{-1}. When the effect of pH was studied, 500 mL of a phosphate buffer solution (8.5 mM) with the desired pH (5 to 11) was used; in these experiments the initial phenol concentration was 150 mg L^{-1}. In all cases ORP, pH, X_{O3}, and Hp were recorded continuously as a function of time. In addition, at predetermined intervals samples were taken to measure chemical oxygen demand (COD) and phenols concentration. COD was determined using the closed reflux colorimetric method in a Hach reactor model DRB200 coupled with a DR/2000 spectrophotometer (Hach Company, Loveland, CO). Total phenols concentration was measured using the Folin−Ciocalteu method.[24]

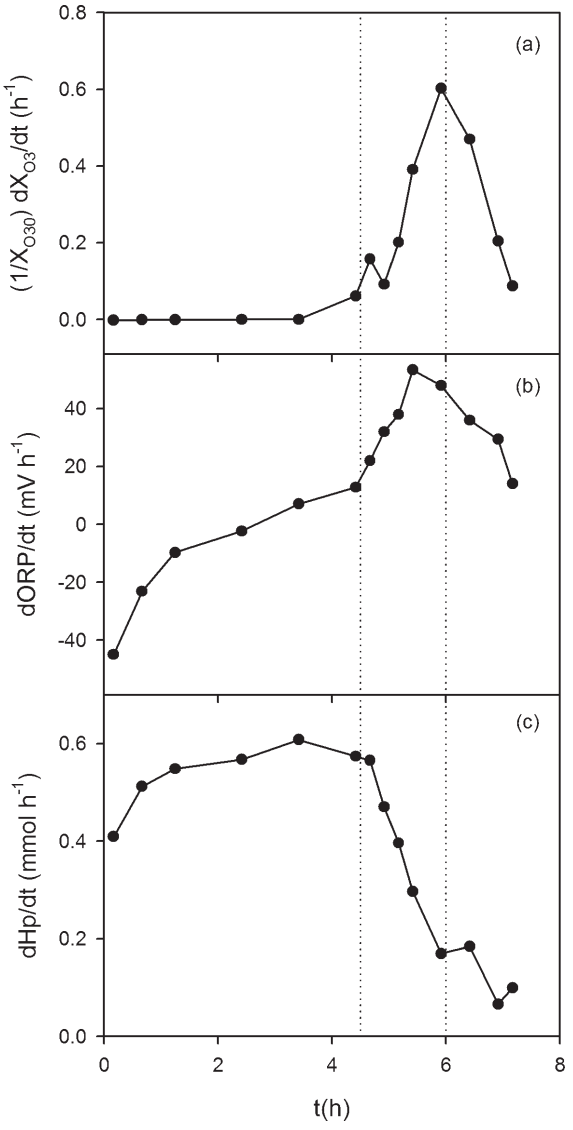

Figure 3. Time profiles of the derivative values of (a) normalized ozone gas outlet concentration ($(1/X_{O30})dX_{O3}/dt$), (b) oxidation−reduction potential ($dORP/dt$), and (c) the proton production rate (dHp/dt). Dotted lines indicate the time interval corresponding to the estimated critical ozonation time.

3. RESULTS AND DISCUSSION

3.1. Relationship Among ORP, Hp, X_{O3}, Phenol, and COD Concentrations During the Ozonation of Phenol Solutions.

Figure 2a shows a typical example of the COD degradation by ozone as a function of time. As it was expected, COD profile exhibited two periods. The first one corresponded to the oxidation of ozone fast-reacting compounds; within this period a linear decrease of COD and phenol concentration was observed. The second period started at about 4.5 to 6.0 h (dotted lines in Figure 2), when COD and phenols concentrations were below 500 and 50 mg L^{-1}, respectively. This second stage was characterized by a COD removal rate that was lower than that corresponding to the first one.

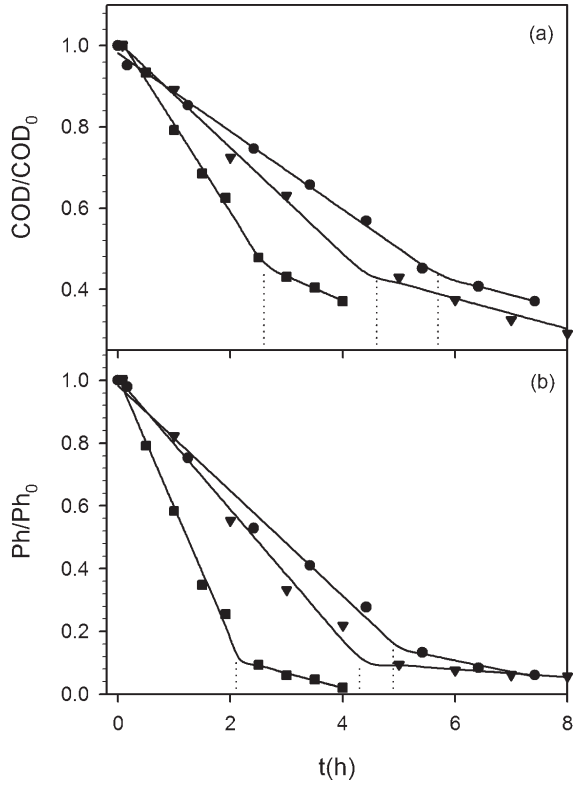

Figure 4. Effect of the initial phenol concentration on the removal of (a) COD, and (b) phenols concentration as a function of the ozonation time. Initial phenol concentrations were (■) 150 mg L^{-1}, (▼) 210 mg L^{-1}, and (●) 420 mg L^{-1}; in all cases pH = 7. Continuous lines indicate the fitting of eq 1 to the experimental data. Dotted lines show the critical ozonation time.

To obtain the critical ozonation time (t_c) based on COD or phenols concentrations (both denoted by C), the following two segment piecewise function was fitted to the values of C as a function of time (t) using the software Sigma Plot 10.0 (Systat Software, Inc.):

$$C = \begin{cases} C_0 - Rt, & 0 \le t \le t_c \\ (C_0 - Rt_c)e^{k(t_c - t)}, & t > t_c \end{cases} \quad (1)$$

where C_0 = initial concentration, R = apparent zero order reaction rate, t_c = critical ozonation time, and k = apparent first order decay rate constant. In eq 1 it was assumed that for $t \le t_c$, the availability of ozone limits the reaction rate; conversely, when C decreases below a certain concentration ($t > t_c$), the reaction rate depends only on C and ozone is in excess. Although rigorous kinetic studies on the ozonation process in bubbled columns were reported,[25,26] eq 1 was accurate enough for the scope of the present paper. For this reason, in order to obtain the critical ozonation time (t_c) based on COD or phenols concentrations (C) eq 1 was used to describe COD and phenols concentrations as a function of the process time.

Taking into account that the critical concentration value (C_C) achieved when $t = t_c$ is $C_c = C_0 - Rt_c$, the normalized critical concentration (C_{CN}) can be calculated as follows:

$$C_{CN} = \frac{C_0 - Rt_c}{C_0} \quad (2)$$

The stoichiometric ratio (z) corresponding to the mass of ozone consumed per unit mass of COD (or phenols) degraded during the first ozonation phase ($t \le t_c$) was calculated by a

Table 1. Effect of the Initial Phenol Concentration (Ph_0) on the Apparent Zero Order Reaction Rate (R), the Normalized Critical Concentration (C_{CN}), the Stoichiometric Coefficient (z), and the Critical Ozonation Time (t_c) Based on Different Measurements

Ph_0 (mg L^{-1})	R^a	C_{CN}	z^b	t_c (h)	measurement
	77.3 ± 2.7	0.45 ± 0.02	1.53 ± 0.09	2.6 ± 0.2	COD
	61.8 ± 2.5	0.11 ± 0.03	1.91 ± 0.12	2.1 ± 0.1	phenol
150				2.5	$(1/X_{O30})dX_{O3}/dt$
				2.2	$dORP/dt$
				1.6	dHp/dt
	59.4 ± 3.5	0.43 ± 0.02	1.98 ± 0.15	4.6 ± 0.7	COD
	43.8 ± 1.6	0.10 ± 0.02	2.69 ± 0.17	4.3 ± 0.2	phenol
210				4.5	$(1/X_{O30})dX_{O3}/dt$
				5	$dORP/dt$
				2.4	dHp/dt
	84.5 ± 6.2	0.44 ± 0.02	1.40 ± 0.08	5.7 ± 0.3	COD
	71.9 ± 2.7	0.15 ± 0.03	1.64 ± 0.10	4.9 ± 0.3	phenol
420				5.2	$(1/X_{O30})dX_{O3}/dt$
				5.5	$dORP/dt$
				4.7	dHp/dt

[a] For COD and phenol measurements, rates R were expressed as mg COD $(L\,h)^{-1}$, and mg phenol $(L\,h)^{-1}$, respectively. [b] z values were expressed as mg O_3 mg COD^{-1}, or mg O_3 mg $phenol^{-1}$.

dx.doi.org/10.1021/ie200999h |Ind. Eng. Chem. Res. 2011, 50, 9799–9809

macroscopic mass balance across the bubble column:[26]

$$z = \frac{F_{O3}}{VR} \quad (3)$$

where F_{O3} = 59 ± 3 $mgO_3\ h^{-1}$ is the inlet gas ozone mass flow rate, and V = 500 mL is the liquid phase volume. To obtain eq 3, it was assumed that the ozone concentration in the outlet gas stream is negligible, thus, a complete consumption of the ozone take place during the first ozonation phase ($t < t_c$).

COD and phenols concentrations as a function of time were fitted to eq 1 in order to obtain the apparent zero order consumption rate (R), and the critical ozonation time (t_c). The critical ozonation time based on COD measurements (t_{cCOD} = 5.7 ± 0.3 h) was close to the calculated value by phenols (t_{cPh} = 4.9 ± 0.3 h). Obtained apparent zero order COD and phenols removal rates were R_{COD} = 84.5 ± 1.7 mg $(L\ h)^{-1}$ and R_{Ph} = 71.9 ± 2.7 mg $(L\ h)^{-1}$, respectively. Taking into account that the theoretical oxygen demand of the oxidation of phenol to CO_2 is 2.38 mg COD mg $Phenol^{-1}$, the ratio R_{COD}/R_{Ph} = 1.18 mg COD mg $phenol^{-1}$ indicates a partial oxidation of phenol during the first ozonation phase. Taking into account the molecular weights of oxygen and phenol, this ratio corresponds to 3.47 mmol of oxygen consumed per mmol of phenol oxidized.

Figure 2b shows that the ozone concentration in the gaseous outlet stream (X_{O3}) was almost zero during the first ozonation period, indicating that the inlet ozone was consumed completely. At t = 4.5 h an increase of X_{O3} was observed; this increment in X_{O3} was associated with the depletion of the ozone fast-reacting compounds. Then, during the second stage of the ozonation process X_{O3} increased, reaching values close to the initial ozone concentration. A similar trend can be observed in Figure 2c with regard to ORP. At the initial time before the addition of phenol and at pH = 7, ORP values were about 850 mV; then, the addition of a pulse of phenol produced a sharp decrease of ORP to values lower than 200 mV. Minimum ORP values were obtained at t = 2.5 h; then, an increase of ORP was observed. Figure 2d shows that the curve corresponding to the proton production (Hp) also exhibited two periods characterized by different proton production rates.

Similar results were reported by other authors. Hsu et al.[11] studied the ozonation of phenol solutions in the presence of calcium salts; those authors found that during the initial stage, the ozone gas outlet concentration was not detectable due to the high reactivity of phenol toward ozone. During this phase, those authors found the accumulation of several intermediates, such as catechol, 1,2,4-benzenetriol, and various organic acids (muconic, malic, fumaric, oxalic). Because these organic acids were less reactive toward ozone, after the depletion of the aromatic compounds, the ozone gas outlet concentration increased and the COD consumption rate decreased. Lan et al.[25] reported that the COD profile during the ozonation of cork-processing water was characterized by a pattern of fast and slow COD depletion rates. Those authors also found that ORP values decreased during the fast COD depletion rate phase followed by an increase of ORP in the slow phase.

To develop online indicators to monitor the ozonation process of phenol-containing wastewaters, the derivative with respect to time of the normalized ozone gas outlet concentration ($(1/X_{O30})dX_{O3}/dt$), of the oxidation−reduction potential (dORP/dt), and of the total proton production (dHp/dt), were plotted as a function of time. Figure 3 shows that the first two indicators exhibited a peak within the estimated range for the

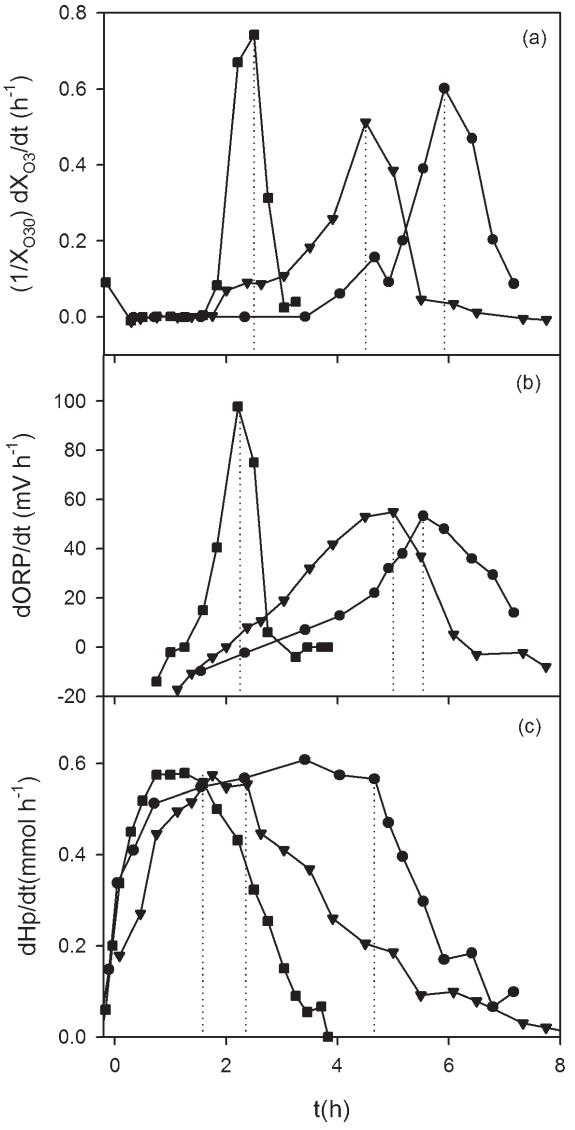

Figure 5. Time profiles of the derivative values of (a) normalized ozone gas outlet concentration ($(1/X_{O30})dX_{O3}/dt$), (b) oxidation−reduction potential (dORP/dt), and (c) the proton production rate (dHp/dt). Initial phenol concentrations were (■) 150 mg L^{-1}, (▼) 210 mg L^{-1}, and (●) 420 mg L^{-1}. In all cases pH = 7. Dotted lines show the critical ozonation time.

critical ozonation time; additionally, a sharp decrease of dHp/dt was also obtained within this range. Thus, in principle, the three indicators could be useful to monitor the ozonation process and to determine the critical ozonation time (t_c). It must be pointed out that t_c can be obtained by fitting the time profile of COD or phenols values to eq 1; however, this procedure is not useful to monitor the ozonation process because it is based on knowledge of the whole curve to determine t_c. On the contrary, the proposed indicators are based on the instantaneous values of X_{O3}, ORP, or Hp; thus, they may provide information concerning the ozonation process on a real time basis.

The use of ORP to monitor the ozonation process has been proposed by other authors.[25,26] These measurements are based on the increase of ORP in the presence of oxidants, such as ozone in water. Because pH is not controlled in most studies concerning the ozonation of wastewaters, the formation of dicarboxylic acids

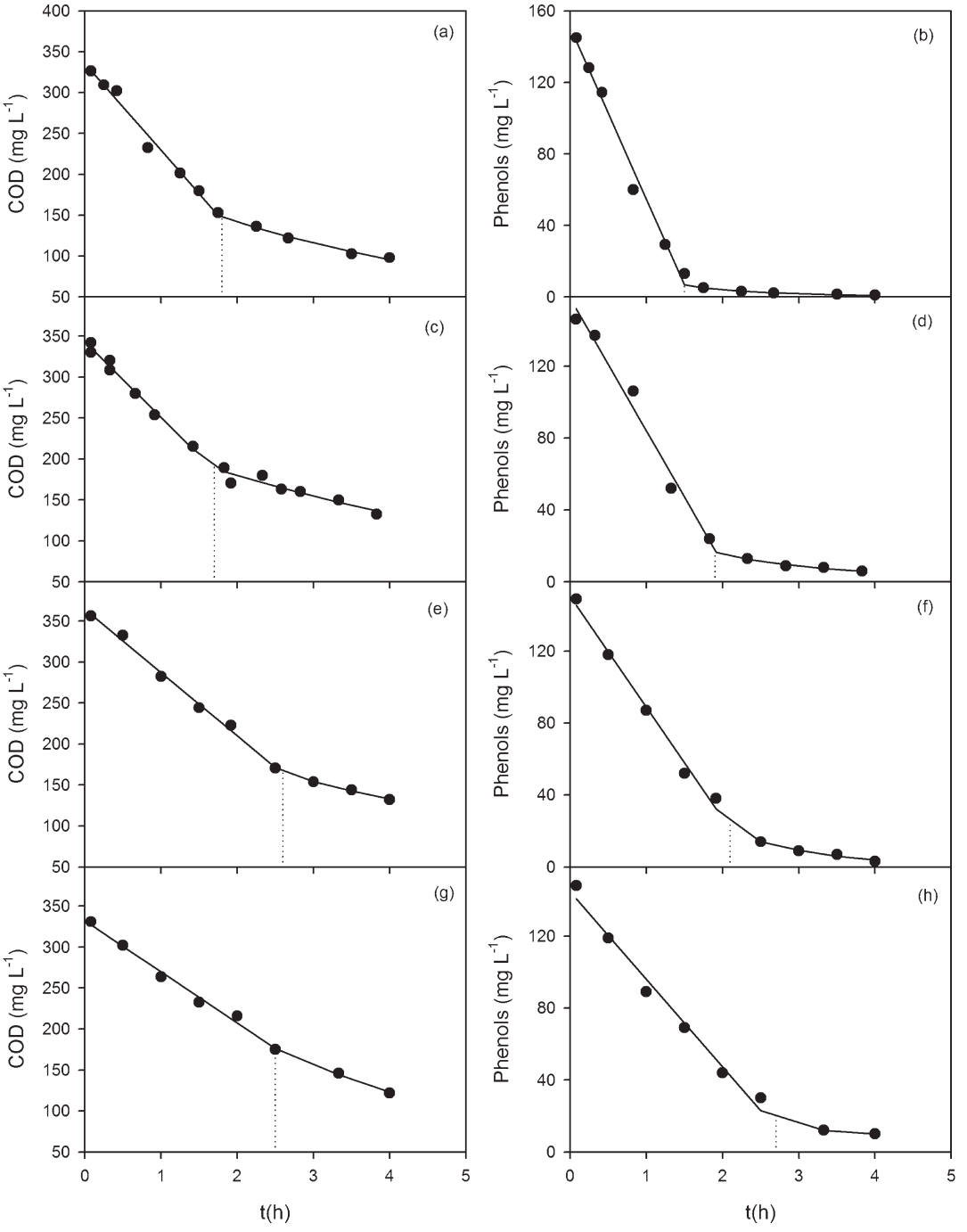

Figure 6. Effect of pH on the removal of COD (a, c, e, g) and phenols (b, d, f, h) during the ozonation of phenol solutions (Ph_0 = 150 mg L^{-1}) at pH 11 (a, b), 9 (c, d), 7 (e, f), and 5 (g, h). Continuous lines indicate the fitting of eq 1 to the experimental data. Dotted lines show the critical ozonation time.

as well as CO_2 produced a decrease of pH during the ozonation process.[25−28] However, it is generally recognized that ORP values are strongly affected by pH;[29] thus, the interpretation of ORP profiles must be evaluated with care. Conversely, in the present work pH was maintained constant; as a result, ORP reflected the oxidation level of the ozonated wastewater and it can be used as a direct indicator of the presence of dissolved ozone.

3.2. Effect of the Initial Phenol Concentration on the Critical Ozonation Time. Ozonation experiments of phenol solutions with different initial phenol concentrations (Ph_0 = 150, 210, or 430 mg L^{-1}) at pH = 7 were performed. Figure 4 shows that in all cases COD, and phenol values as a function of time, exhibited the typical profile corresponding to the ozonation of phenol solutions: a first fast reaction period followed by a second slower step. Equation 1 was fitted to the data shown in Figure 4 to obtain the zero order rate (R), and the critical ozonation time (t_c) based on COD and phenols concentrations. Table 1 shows that no trend can be noticed with regard to the effect of the initial phenol concentration on the apparent zero order reaction rate based on COD or phenols measurements (R_{COD}, R_{Ph}). From these data, the calculated R_{COD}/R_{Ph} ratio was 3.7 ± 0.6 mmol of oxygen consumed per mmol of phenol oxidized.

dx.doi.org/10.1021/ie200999h |*Ind. Eng. Chem. Res.* 2011, 50, 9799–9809

The linear depletion of COD and phenols during the first ozonation step indicates that the phenol oxidation rate was limited by the inlet mass flow of ozone; therefore, the critical ozonation time (t_c) increased with higher initial phenol concentrations (Ph_0). Conversely, the normalized critical concentration (C_{CN}) was almost constant for all the tested Ph_0 values; the overall mean C_{CN} corresponding to COD and phenols were 0.45 ± 0.01, and 0.14 ± 0.07, respectively. The normalized critical concentration (C_{CN}) may be utilized as an indicator of the phase during the ozonation process. For example, if the ratio $COD/COD_0 < 0.45$, it can be considered that the second phase of the ozonation process was achieved. Table 1 also shows the mass of ozone consumed per unit mass of COD (or phenols) degraded (z) during the first ozonation phase; similarly to R, no trend can be noticed with regard to the effect of the initial phenol concentration on the stoichiometric coefficient z.

Figure 5 shows the derivative with respect to time of the normalized ozone gas outlet concentration ($(1/X_{O30})dX_{O3}/dt$), the oxidation−reduction potential ($dORP/dt$), and the proton production rate (dHp/dt) as a function of time corresponding to different initial phenol concentrations. Maximum values corresponding to $(1/X_{O30})dX_{O3}/dt$ and $dORP/dt$ were reached at a time close to the critical ozonation time; in addition, a sharp decrease of dHp/dt values was also observed. Table 1 shows that for all the tested initial phenol concentrations, the critical ozonation time based on maximum values of $(1/X_{O30})dX_{O3}/dt$ and $dORP/dt$ was close to the average values obtained using COD or phenols measurements. Conversely, critical ozonation times determined through dHp/dt values corresponding to Ph_0 = 150 and 210 mg L^{-1} were about half the average values based on COD or phenols measurements, suggesting that dHp/dt may not a suitable indicator to monitor the ozonation process.

3.3. Effect of pH on the Determination of the Critical Ozonation Time. Ozonation of phenol solutions at different pH (pH = 5, 7, 9, 11) were performed; in these experiments the initial phenol concentration was 150 mg L^{-1}. Figure 6 shows that in all cases time profiles corresponding to COD and phenol concentrations exhibited the typical two reaction phases. Equation 1 was fitted to the data shown in Figure 6 to obtain the apparent zero order reaction rate (R), and the critical ozonation time (t_c). Table 2 shows that R_{COD} and R_{Ph} increased with higher pH values; as a result, t_c values decreased as pH increase. However, the ratio R_{COD}/R_{Ph} was almost constant as a function of pH. The overall mean R_{COD}/R_{Ph} ratio was 3.6 ± 0.4 mmol of oxygen consumed per mmol of phenol oxidized; this value is in agreement with the R_{COD}/R_{Ph} ratio calculated in the previous section.

With reference to the effect of pH on the normalized critical concentration (C_{CN}), no trend can be noticed in Table 2. For all the tested pH values, the overall mean C_{CN} based on COD and phenols measurements were 0.49 ± 0.09, and 0.10 ± 0.02, respectively; these values are close to the value obtained in the previous section (0.45 ± 0.01, and 0.14 ± 0.07). Table 2 also shows that the mass of ozone consumed per unit mass of COD (or phenols) degraded during the first ozonation phase (z) decreased as pH increased. Thus, the utilization of ozone to remove COD was more efficient at alkaline conditions. This effect can be explained taking into account that ozone oxidizes

Table 2. Effect of pH on the Apparent Zero Order Reaction Rate (R), the Normalized Critical Concentration (C_{CN}), the Stoichiometric Coefficient (z), and the Critical Ozonation Time (t_c) Based on Different Measurements

pH	R^a	C_{CN}	z^b	t_c (h)	measurement
	62.4 ± 4	0.53 ± 0.10	1.89 ± 0.16	2.5 ± 0.5	COD
	48.7 ± 3.2	0.09 ± 0.15	2.42 ± 0.20	2.7 ± 0.4	phenol
				2.3	$(1/X_{O30})dX_{O3}/dt$
5				2.0	$dORP/dt$
					$dLog(ORP)/dt$
					dHp/dt
	77.2 ± 2.6	0.45 ± 0.05	1.53 ± 0.09	2.6 ± 0.2	COD
	61.8 ± 2.9	0.14 ± 0.09	1.91 ± 0.13	2.1 ± 0.2	phenol
				2.5	$(1/X_{O30})dX_{O3}/dt$
7				2.5	$dORP/dt$
				2.5	$dLog(ORP)/dt$
					dHp/dt
	92.2 ± 4.2	0.54 ± 0.04	1.28 ± 0.09	1.7 ± 0.1	COD
	73.7 ± 2.6	0.11 ± 0.06	1.60 ± 0.10	1.9 ± 0.1	phenol
				2.3	$(1/X_{O30})dX_{O3}/dt$
9				1.8	$dORP/dt$
				1.8	$dLog(ORP)/dt$
				1.8	dHp/dt
	106.1 ± 4.7	0.43 ± 0.04	1.11 ± 0.08	1.8 ± 0.1	COD
	96.3 ± 4.0	0.04 ± 0.08	1.23 ± 0.08	1.5 ± 0.1	phenol
				2.1	$(1/X_{O30})dX_{O3}/dt$
11				1.4	$dORP/dt$
				1.2	$dLog(ORP)/dt$
				1.1	dHp/dt

[a] For COD and phenol measurements, rates R were expressed as mg COD $(L\,h)^{-1}$, and mg phenol $(L\,h)^{-1}$, respectively. [b] z values were expressed as mg O_3 mg COD^{-1}, or mg O_3 mg $phenol^{-1}$.

dx.doi.org/10.1021/ie200999h |*Ind. Eng. Chem. Res.* 2011, 50, 9799–9809

the organic matter via direct or indirect reactions. In the first steps, the direct reaction of ozone with phenol produces catechol (or *p*-hydroquinone) and molecular oxygen.[9,11] Then, these products react with ozone to obtain other more oxidized compounds and carbon dioxide. The formation of molecular oxygen reduces the utilization efficiency of ozone, yielding higher values of *z*. Ozone can also react with organic matter via hydroxyl and other radicals that are generated during the ozone decomposition in water. This reaction, and therefore the formation of radicals, is favored under alkaline conditions; thus, at pH values higher than 7 indirect reactions prevail over direct ones.[5−8] Results shown in Table 2 indicate that the utilization efficiency of ozone in the indirect reactions is higher than the efficiency corresponding to the direct ones.

Numerous oxidation products and reaction pathways of the ozonation of phenol solutions have been reported.[9,13,14,30,31] Phenol oxidation can take place at *para* or *ortho*-positions. The oxidation of phenol at the *para*-position generates *p*-benzoquinone which can be further oxidized to give 2,5-dioxo-3-hexenedioic acid; then, the oxidation and decarboxylation of this acid gives maleic acid ($C_4H_4O_4$).[32] This process can be summarized as follows:

$$C_6H_6O + 4O_2 \rightarrow C_4H_4O_4 + 2CO_2 + H_2O \quad (4)$$

Muconic acid ($C_6H_6O_4$) is generated by the oxidation of phenol via the *ortho*-position. Muconic acid can be further oxidized to give a mixture of carbon dioxide and 4-oxo-2-butenoic ($C_4H_4O_3$), formic (CH_2O_2), glyoxylic ($C_2H_2O_3$), and maleic ($C_4H_4O_4$) acids:[14]

$$C_6H_6O + 3O_2 \rightarrow CH_2O_2 + C_4H_4O_3 + CO_2 \quad (5)$$

$$C_6H_6O + 3O_2 \rightarrow C_2H_2O_3 + C_4H_4O_4 \quad (6)$$

If the oxidation process continues, 4-oxo-2-butenoic acid gives glyoxylic and oxalic acids, and eventually CO_2 and formic. Maleic acid can also be further oxidized to give the above-mentioned organic acids, as well as acrylic and acetic acids.[14,32]

In the present work, it was demonstrated that 3.6 ± 0.4 mmol of oxygen was consumed per mmol of phenol oxidized during the first ozonation phase. This result suggests that within the tested conditions, the first reaction step ends after the aromatic ring cleavage and partial oxidation of the intermediate products. If this process can be represented by eq 4, 4 mmol of oxygen would be needed to oxidize phenol to maleic acid. However, eqs 5 and 6 show that in both cases, only 3 mmol of oxygen is consumed per mmol of phenol oxidized. The oxygen consumption obtained in the present work (3.6 ± 0.4 mmol O_2 mmol Ph^{-1}) indicates that 60% of phenol was oxidized via the *para*-position (eq 4), and 40% via the *ortho*-position (eqs 5, 6). This result is close to the reported by Ramseier and von Gunten[14] with regard to the ozonation of a phenol soultion at pH 7.

Figures 7, 8, and 9 show the derivative with respect to time of the normalized ozone gas outlet concentration ($(1/X_{O30})dX_{O3}/dt$), the oxidation−reduction potential and its logarithmic value (dORP/d*t*, dLog(ORP)/d*t*), and the proton production rate (dHp/d*t*) as a function of time, respectively. From these data, t_c

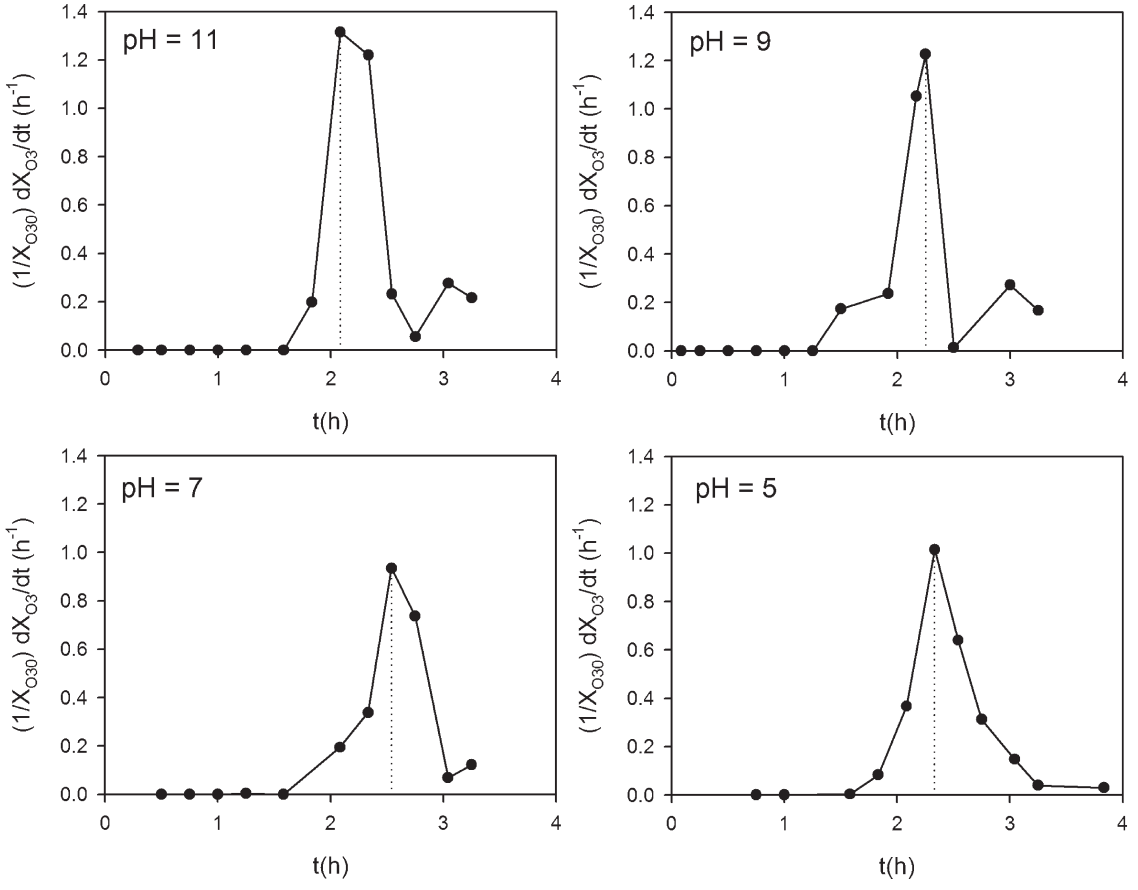

Figure 7. Time profiles of the derivative values of the normalized ozone gas outlet concentration ($(1/X_{O30})dX_{O3}/dt$) during the ozonation of a phenol solution (Ph_0 = 150 mg L^{-1}) at different pH values. Dotted lines show the critical ozonation time.

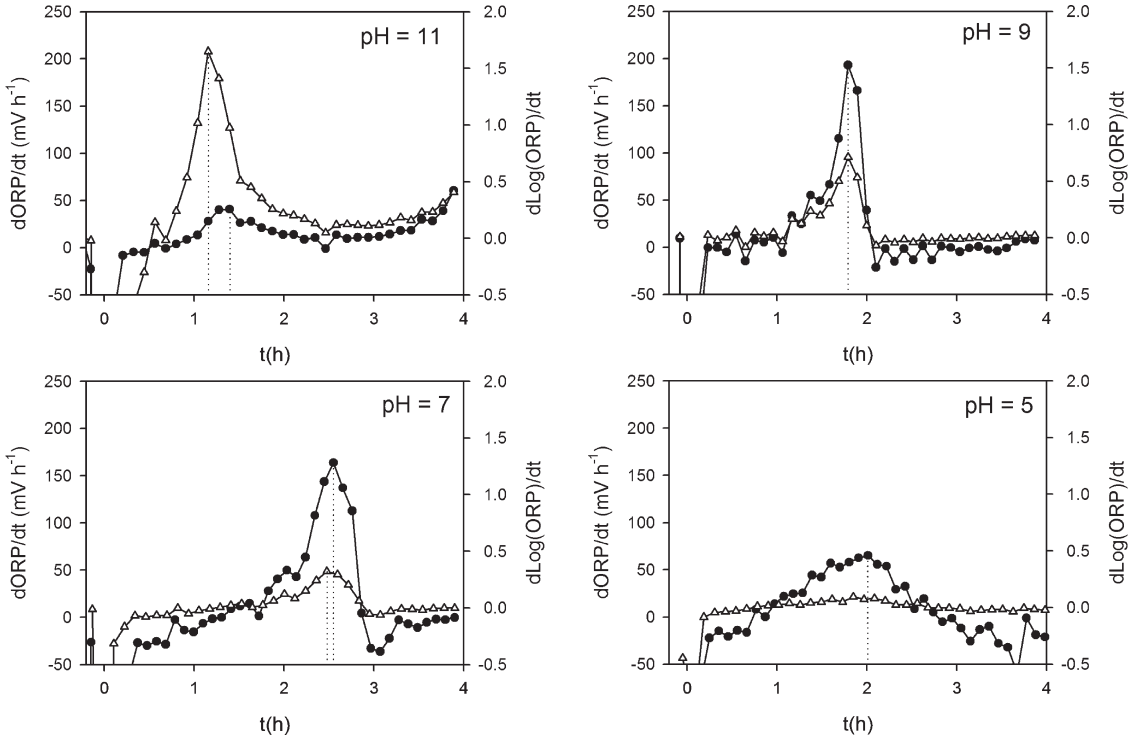

Figure 8. Time profiles of the derivative values of ORP (●) and Log(ORP) (▲) during the ozonation of a phenol solution (Ph_0 = 150 mg L^{-1}) at different pH values. Dotted lines show the critical ozonation time.

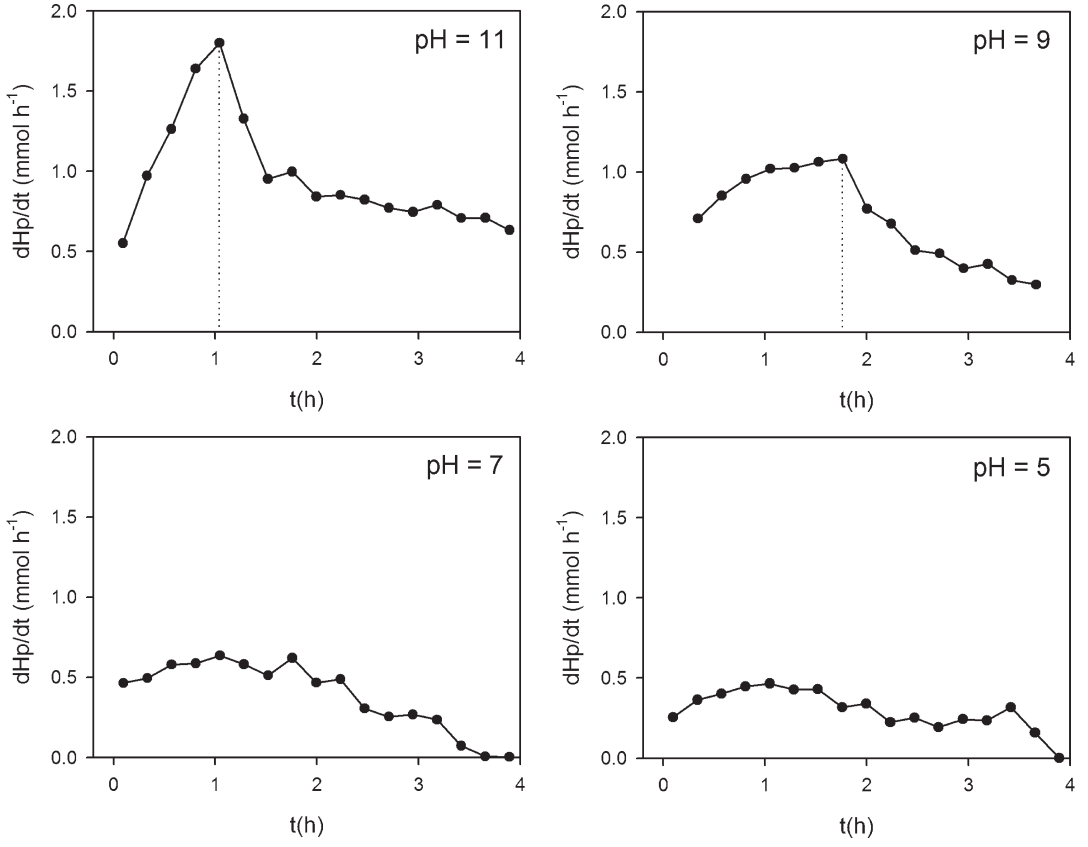

Figure 9. Time profiles of the proton production rate (dHp/d*t*) during the ozonation of a phenol solution (Ph_0 = 150 mg L^{-1}) at different pH values. Dotted lines show the critical ozonation time.

dx.doi.org/10.1021/ie200999h |*Ind. Eng. Chem. Res.* 2011, 50, 9799–9809

values corresponding to the different tested pH values were obtained. Table 2 shows that, in general, t_c values decreased as the pH increased; additionally, these values are in good agreement with those obtained based on COD or phenol measurements. For all the tested pH the indicator $(1/X_{O30})dX_{O3}/dt$ exhibited a clear maximum, from which t_c values were easily obtained (Figure 7). However, not all indicators were applicable in all cases. Figure 8 shows that at pH 11 the curve $dORP/dt$ as a function of time had poor defined maximum value; at this pH, a better estimation of t_c can be obtained from the time profile of $dLog(ORP)/dt$. Additionally, both indicators can be used to determine t_c at pH = 9; however, only $dORP/dt$ exhibited a clear maximum at pH 5 and 7 (Figure 8).

Figure 9 and Table 2 show that the proton production rate (dHp/dt) can be used to determine t_c only for pH values higher than 9. Additionally, Figure 9 shows that the maximum dHp/dt increased as pH increased. The proton production rate is a function of all reactions that affect pH, such as the formation and consumption of organic acids, and the CO_2 formed during the ozonation of phenol.[12] With regard to CO_2, the net proton production results from the balance between the formation and hydration of CO_2, and its stripping from the aqueous phase, which depends on the apparent CO_2 volumetric mass transfer coefficient. Previous studies show that this coefficient decreases about 2 orders of magnitude when pH increases from 6.5 to 8.4; at pH values higher than 9 the CO_2 stripping process in the bubble column used in the present work is negligible.[23] Under these conditions, almost all the CO_2 formed during the ozonation of phenol produces HCO_3^- and H^+; for this reason, the proton production rate increased as pH increased (Figure 9).

4. CONCLUSION

Oxidation−reduction potential (ORP) and proton production (Hp) profiles can be used as alternative indicators to monitor the ozonation of phenol solutions at constant pH. Analysis of the ozone gas outlet stream (X_{O3}), COD, and phenol measurements in the aqueous phase confirm the reliability of the proposed methods. The derivative with respect to time of the normalized ozone gas outlet concentration ($(1/X_{O30})dX_{O3}/dt$), the oxidation−reduction potential ($dORP/dt$) or its logarithmic value ($dLog(ORP)/dt$), and the proton production rate (dHp/dt) exhibited maximum values close to the critical ozonation time (t_c). However, while ORP and X_{O3} measurements were useful to determine t_c for all the tested pHs (5 to 11), Hp values can be used to determine t_c only for pH values higher than 9. The indicators of the ozonation process proposed in the present work (ORP and Hp) as alternatives of X_{O3} may be useful to control the addition of ozone, minimizing the ozonation process costs. Feasibility studies of these indicators to monitor the ozonation of actual phenol containing wastewaters are necessary.

AUTHOR INFORMATION

Corresponding Author

*E-mail: edgardo.contreras@ing.unlp.edu.ar.

ACKNOWLEDGMENT

We gratefully acknowledge the financial support given by Universidad Nacional de La Plata (UNLP), Consejo Nacional de Investigaciones Científicas y Técnicas (CONICET), Agencia Nacional de Promoción Científica y Tecnológica Argentina (ANPCyT), and Monsanto Argentina.

NOMENCLATURE

C = COD or phenols concentration, mg L^{-1}
C_{CN} = normalized critical concentration, dimensionless
C_0 = initial COD or phenols concentration, mg L^{-1}
COD = chemical oxygen demand
F_{O3} = ozone mass flow rate, mg O_3 h^{-1}
Hp = proton production, mmol
k = apparent first order decay rate constant, h^{-1}
ORP = oxidation−reduction potential, mV
Ph_0 = initial phenol concentration, mg L^{-1}
R = apparent zero order reaction rate, mg (L h) $^{-1}$
t_c = critical ozonation time, h
X_{O3} = ozone concentration in the gaseous outlet stream, ppm (v/v)
z = stoichiometric ratio, mg O_3 mg COD^{-1} or mg O_3 mg Ph^{-1}

REFERENCES

(1) USEPA. *Toxicological Review. Phenol. CAS No. 108-95-2*; U.S. Environmental Protection Agency: Washington DC, 2000.

(2) Gogate, P. R.; Pandit, A. A review of imperative technologies for wastewater treatment. I: Oxidation technologies at ambient conditions. *Adv. Environ. Res.* **2004**, *8*, 501.

(3) Gogate, P. R.; Pandit, A. A review of imperative technologies for wastewater treatment. II: Hybrid methods. *Adv. Environ. Res.* **2004**, *8*, 553.

(4) Langlais, B.; Reckhow, D. A.; Brink, D. R. *Ozone in Water Treatment: Application and Engineering*; Lewis Publisher: Chelsea, MI, 1991.

(5) Buhler, R. E.; Staehelin, S.; Hoigné, J. Ozone decomposition in water studied by pulse radiolysis. 1. OH_2/O_2^- and HO_3/O_3^- as intermediates. *J. Phys. Chem.* **1984**, *88*, 2560.

(6) Staehelin, S.; Buhler, R. E.; Hoigné, J. Ozone decomposition in water studied by pulse radiolysis. 2. OH and OH_4 as chain intermediates. *J. Phys. Chem.* **1984**, *88*, 5999.

(7) Tomiyasu, H.; Fukutomi, H.; Gordon, G. Kinetics and mechanism of ozone decomposition in basic aqueous solution. *Inorg. Chem.* **1985**, *24*, 2962.

(8) Fabian, I. Reactive intermediates in aqueous ozone decomposition: A mechanistic approach. *Pure Appl. Chem.* **2006**, *78*, 1559.

(9) Villaseñor, J.; Reyes, P.; Pecchi, G. Catalytic and photocatalitic ozonation of phenol on MnO_2 supported catalysts. *Catal. Today* **2002**, *76*, 121.

(10) Hammes, F.; Salhi, E.; Köster, O.; Kaiser, H. P.; Egli, T.; von Gunten, U. Mechanistic and kinetic evaluation of organic disinfection by-product and assimilable organic carbon (AOC) formation during the ozonation of drinking water. *Water Res.* **2006**, *40*, 2275.

(11) Hsu, Y. C.; Chen, J. H.; Yang, H. C. Calcium enhanced COD removal for the ozonation of phenol solution. *Water Res.* **2007**, *41*, 71.

(12) Beltrán, F. J. *Ozone Reaction Kinetics for Water and Wastewater Systems*; CRC Press LLC, Lewis Publishers, 2004.

(13) Roig, B.; Gonzalez, C.; Thomas, O. Monitoring of phenol photodegradation by ultraviolet spectroscopy. *Spectrochi. Acta Part A* **2003**, *59*, 303.

(14) Ramseier, M. K.; von Gunten, U. Mechanisms of Phenol Ozonation - Kinetics of Formation of Primary and Secondary Reaction Products. *Ozone Sci. Eng.* **2009**, *31*, 201.

(15) Silva, G. H. R.; Daniel, L. A.; Bruning, H.; Rulkens, W. H. Anaerobic effluent disinfection using ozone: Byproducts formation. *Bioresour. Technol.* **2010**, *101*, 6981.

(16) Petala, M.; Samaras, P.; Zouboulis, A.; Kungolos, A.; Sakellaropoulos, G. P. Influence of ozonation on the in vitro mutagenic and toxic potential of secondary effluents. *Water Res.* **2008**, *42*, 4929.

(17) Amat, A. M.; Arques, A.; Beneyto, H.; García, A.; Miranda, M. A.; Seguí, S. Ozonisation coupled with biological degradation for treatment of phenolic pollutants: A mechanistically based study. *Chemosphere* **2003**, *53*, 79.

(18) Benitez, F. J.; Acero, J. L.; Garcia, J.; Leal, A. I. Purification of cork processing wastewaters by ozone, by activated sludge, and by their two sequential applications. *Water Res.* **2003**, *37*, 4081.

(19) Ebeling, D.; Patel, V.; Findlay, M.; Stetter, J. Electrochemical ozone sensor and instrument with characterization of the electrode and gas flow effects. *Sens. Actuators B* **2009**, *137*, 129.

(20) Rakness, K.; Gordon, G.; Langlais, B.; Masschelein, W.; Matsumoto, N.; Richard, Y.; Robson, C. M.; Somiya, I. Guideline for measurement of ozone concentration in the process gas from an ozone generator. *Ozone Sci. Technol.* **1996**, *18*, 209.

(21) Bendahan, M.; Boulmani, R.; Seguin, J. L.; Aguir, K. Characterization of ozone sensors based on WO3 reactively sputtered films: Influence of O_2 concentration in the sputtering gas, and working temperature. *Sens. Actuators B* **2004**, *100*, 320.

(22) Knake, R.; Jacquinot, P.; Hodgeson, A.; Hauser, P. Amperometric sensing in the gas-phase. *Anal. Chim. Acta* **2005**, *549*, 1.

(23) Contreras, E. M. Carbon dioxide stripping in bubbled columns. *Ind. Eng. Chem. Res.* **2007**, *46*, 6332.

(24) Tziotzios, G.; Teliou, M.; Kaltsouni, V.; Lyberatos, G.; Vayenas, D. V. Biological phenol renoval using suspended growth and packed bed reactors. *Biochem. Eng. J.* **2005**, *26*, 65.

(25) Lan, B. Y.; Nigmatullin, R.; Puma, G. L. Ozonation kinetics of cork-processing water in a bubble column reactor. *Water Res.* **2008**, *42*, 2473.

(26) Lucas, M. S.; Peres, J. A.; Lan, B. Y.; Puma, G. L. Ozonation kinetics of winery wastewater in a pilot-scale bubble column reactor. *Water Res.* **2009**, *43*, 1523.

(27) Lucas, M. S.; Peres, J. A.; Puma, G. L. Treatment of winery wastewater by ozone-based advanced oxidation processes (O_3, O_3/UV, and O_3/UV/H_2O_2) in a pilot-scale bubble column reactor and process economics. *Sep. Purif. Technol.* **2010**, *72*, 235.

(28) de Souza, S. M. d. A. G. U.; Bonilla, K. A. S.; de Souza, A. A. U. Removal of COD and color from hydrolyzed textile azo dye by combined ozonation and biological treatment. *J. Hazard. Mater.* **2010**, *179*, 35.

(29) Stumm, W.; Morgan, J. J. *Aquatic Chemistry*, 3rd ed.; Wiley: New York, 1996.

(30) Mvula, E.; von Sonntag, C. Ozonolysis of phenols in aqueous solution. *Org. Biomol. Chem.* **2003**, *1*, 1749.

(31) Komissarov, V. D.; Zimin, Y. S.; Khursan, S. L. On the Mechanism of Phenol Ozonolysis. *Kinet. Catal.* **2006**, *47*, 850.

(32) Devlin, H. R.; Harris, I. J. Mechanism of the Oxidation of Aqueous Phenol with Dissolved Oxygen. *Ind. Eng. Chem. Fundam.* **1984**, *23*, 387.